

Virtual Thin Slice: 3D Conditional GAN-based Super-resolution for CT Slice Interval

Akira Kudo¹, Yoshiro Kitamura¹, Yuanzhong Li¹, Satoshi Iizuka², and Edgar Simo-Serra³

¹ Imaging technology center, Fujifilm corporation, Minato, Tokyo, Japan

² Center for Artificial Intelligence Research, University of Tsukuba, Tsukuba, Ibaraki, Japan

³ Department of computer science and engineering, Waseda university, Shinjuku, Tokyo, Japan

akira.kudo@fujifilm.com

Abstract. Many CT slice images are stored with large slice intervals to reduce storage size in clinical practice. This leads to low resolution perpendicular to the slice images (*i.e.*, z-axis), which is insufficient for 3D visualization or image analysis. In this paper, we present a novel architecture based on conditional Generative Adversarial Networks (cGANs) with the goal of generating high resolution images of main body parts including head, chest, abdomen and legs. However, GANs are known to have a difficulty with generating a diversity of patterns due to a phenomena known as mode collapse. To overcome the lack of generated pattern variety, we propose to condition the discriminator on the different body parts. Furthermore, our generator networks are extended to be three dimensional fully convolutional neural networks, allowing for the generation of high resolution images from arbitrary fields of view. In our verification tests, we show that the proposed method obtains the best scores by PSNR/SSIM metrics and Visual Turing Test, allowing for accurate reproduction of the principle anatomy in high resolution. We expect that the proposed method contribute to effective utilization of the existing vast amounts of thick CT images stored in hospitals.

Keywords: Deep Learning · Generative Adversarial Network · Super Resolution · Computer Vision · Computed Tomography.

1 Introduction

Image diagnosis plays an important role in recent healthcare solutions. The quality of diagnostic images largely affects the quality of diagnosis. The images such as CT or MRI acquired in hospitals are normally stored in Picture Archiving and Communication Systems (PACS). Although thin slice images, with slice intervals are about less than 1 mm, are frequently used for diagnosis, thick slice images with large slice intervals are used for long term storage to reduce the data size. However, the stored thick slice images do not have sufficient resolution for

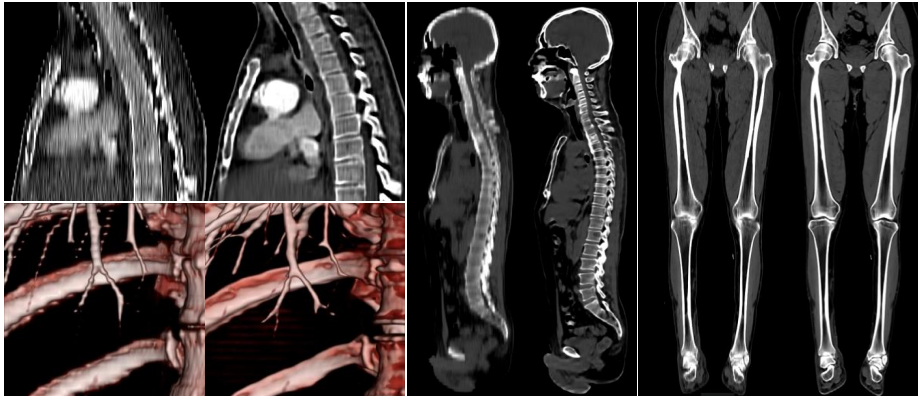


Fig. 1. Comparison of original thick image and the virtual thin image output generated by the proposed approach. On the left top row, the CT sagittal view of original thick image is blurred with each vertebrae bone being nearly indistinguishable, while they become clear in corresponding $\times 8$ super resolution image (Virtual Thin). Arbitrary size data, even the whole body shown on the right, is available for inputs and capable of reconstructing natural image regardless of body part. On the left bottom row, fine blood vessel are smoothly reconstructed in a volume rendering view.

sagittal or coronal views, and also have limited applicability to 3D visualization (volume rendering). To address this, we present a novel super resolution algorithm for CT images based on Generative Adversarial Networks (GAN). Our goal is to generate high resolution 3D images corresponding from the input thick slice images. We base our approach on adversarial training [5] and aim to generate realistic-looking high-resolution CT images. One of the major difficulties is that CT images can be very diverse (*e.g.*, imaged body part, voxel size, resolution, slice thickness, slice interval, etc), which can be difficult to synthesize with GANs. This difficulty is due to a phenomena known as mode collapse, in which the model becomes only able to synthesize a small subset of the original training data and presents a significant decrease in the output diversity [9]. We overcome this issue by additional conditioning of the discriminator on additional information, and use a three dimensional fully convolutional network to synthesize the high resolution CT images. Figure 1 shows example input thick images and the corresponding thin images synthesized by the proposed Virtual Thin Slice (VTS) method. The vertebrae bone structure is clearly reconstructed on the sagittal view, and fine blood vessels are reproduced well on the VR image.

2 Related work

Single image super resolution is a major problems in computer vision field with a long history. The very first approach were filtering approaches, such as linear, bicubic or Lanczos filtering [4] which do not require huge computation. Yang et al. [14] categorized super resolution technique into 4 groups, which are prediction models, edge-based methods, image statistical methods and path-based

methods. Recently, deep convolutional neural networks (CNN) based methods are showing significant performance in image recognition area [11]. SRCNN [3] improved performance on 2D image super resolution tasks by training non-linear low-resolution to high-resolution mappings using CNN filters. This is achieved through the minimization of pixel-wise Mean Squared Error (MSE) between reconstructed image and ground truth high resolution image. However, pixel-wise losses cannot capture perceptual differences [1], thus the output tends to be blurred and look unrealistic to human eyes. Adversarial training schemes [5] give much sharper result in image conversion task. Our work builds upon adversarial training to obtain better results. Some research focus on stabilize GAN training to reduce mode collapse, while there is a drawback of the computational cost [9].

Conditional GAN [10] is a conditioned min-max game between generator and discriminator. Isola [7] proposed Pix2Pix algorithm using images as conditional information, using pair of input image and target ground truth image. While adversarial approach gives more adequate to human perception, there are trade-offs between the perception and distortion of generating images [8].

In medical imaging, few researchers work on the 3D image super resolution. Chen et al. targeted 3D MRI super-resolution for medical image analysis [2]. Their target was limited to brain images. One of our contributions is realizing 3D CT image super resolution for any kind of body parts with a single generator network. Another contribution is the conditioning of the discriminator on the different body parts inspired by conditional GAN, and the ability to perform super-resolution of 3D medical images of arbitrary sizes.

3 Method

3.1 Objective Function

Our approach is based on conditional GAN, using pairs of low resolution data and high resolution data with slice information. The objective is to learn the transformation from of the thick slice image x to the virtual thin slice image y . Additionally, the discriminator is condition on a vector w , allowing the objective function to be expressed as

$$L_{cGAN}(G, D) = E_{(x,y)} [\log D(x, y, w)] + E_x [\log(1 - D(x, G(x), w))]. \quad (1)$$

where the model G tries to minimize this objective against an adversarial model D that tries to maximize it. Both G and D can be implemented as Convolutional Neural Networks (CNN). We also use a L_1 loss to calculate pixel-wise appearance differences between ground truth images and generated images, which has been shown to give less blurring than the L_2 loss in a diversity of image-to-image translation tasks [7]. Therefore, our final objective is expressed as

$$G^* = \arg \min_G \max_D L_{cGAN}(G, D) + \lambda L_{L1}(G) \quad (2)$$

Figure 2 illustrates the proposed adversarial training procedure. Note that the additional conditions are not inputted into the generator.

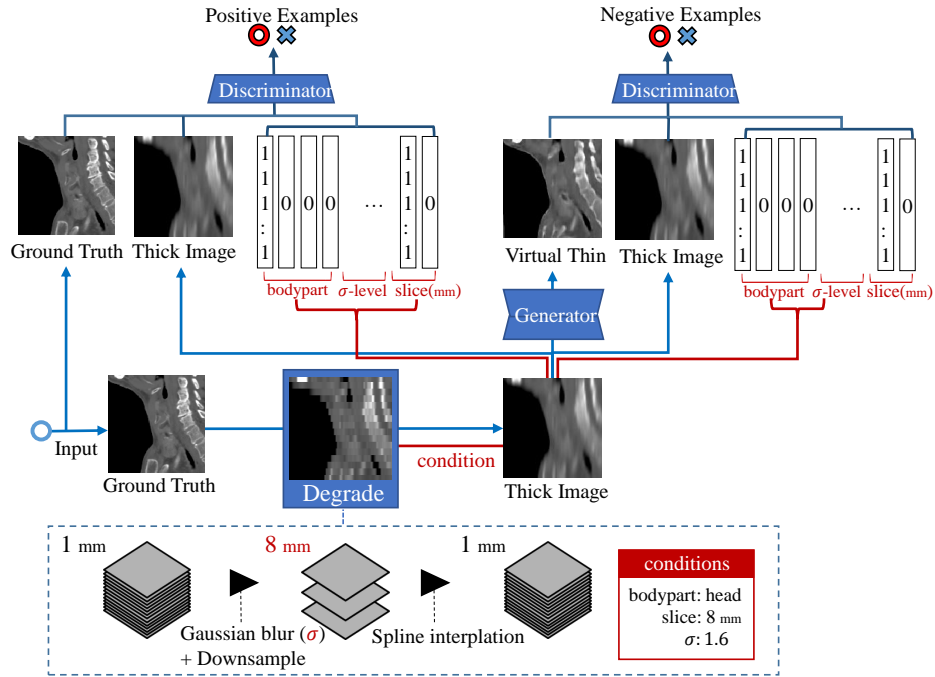


Fig. 2. Adversarial training framework of thick-thin slice translation on CT images. In each training iteration, the thin slice input data is randomly degraded to simulate thick slice data. For the Generator input, we feed 1 mm spline interpolated 3D thick slice image itself. On the other hand, for the Discriminator input, we feed generated Virtual Thin image with slice condition including body part information with degraded parameter scales.

3.2 Network Architecture

Both our generator and discriminator models are based on Convolutional Neural Networks. Each convolutional layer consists of $4 \times 4 \times 4$ sized kernel followed by batch normalization [6] and LeakyReLU ($\alpha = 0.2$) as the activation function. Instead of max-pooling, strided convolution are used and image resolution is reduced to $1/2$ in each encoder convolutional layer. We set 64 channels for the first layer for both of the generator and the discriminator to get sufficient quality results and acceptable computation time. Figure 3 illustrates the architecture of our generator and discriminator networks.

Generator The generator uses an encoder-decoder type architecture inspired by U-Net [12]. The resolution is decreased 4 times such that the minimum feature map size is $1/16$, and restored to the original size with trilinear interpolation. We used trilinear interpolation instead of transposed convolution for up-sampling to avoid generating checkered patterns due to uneven overlap of the kernel.

In each convolutional layer, more feature channels generate better results, but require more resources and computational time. The generator estimates the high frequency components and the output is finally added to the input image.

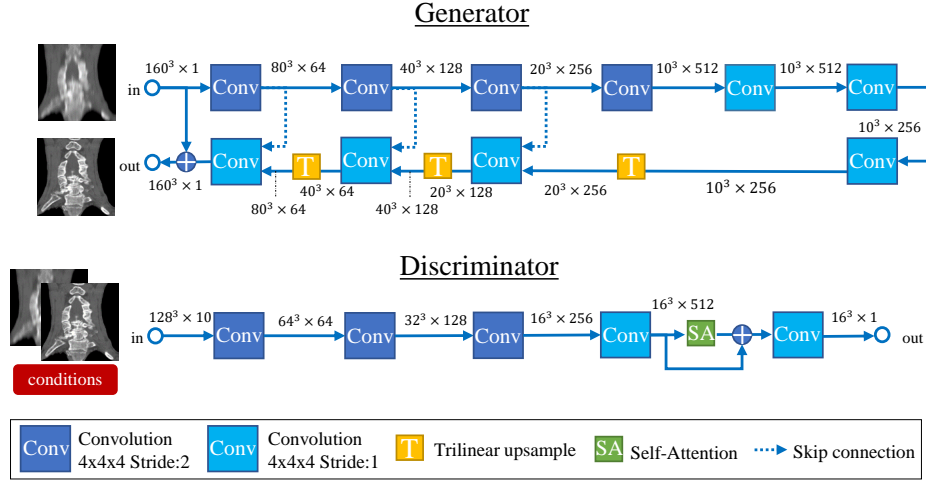


Fig. 3. Overview of the generator and discriminator network architectures. $(x^3 \times c)$ denotes the size of 3D feature map volumes, where c denotes the number of channels.

Discriminator For the discriminator input, thick image (1 channel), thin image (1 channel) and slice information (8 channels) is given. Also a self-attention layer [15] is added in the fourth layer of the network. Self-attention mechanism is an idea to introduce global information between layers by computing attention maps which show the relevant area. In our case, self-attention did not largely affect the final performance, however, it speeded up the convergence of adversarial training. Final output is converted to a probability with a Sigmoid function.

3.3 Training data

We introduce a Degradar procedure to randomly degrade the original thin image to thick slice image. In the Degradar, the input 3D image is down-sampled with Gaussian smoothing and spline interpolation is used to generate the missing slices. To simulate various combination of slice thickness and slice interval, the number of slices is reduced to either $1/4$ or $1/8$, then spline interpolation and random Gaussian noise is applied. The training samples are randomly cropped from the training images with an affine transform.

3.4 Conditioning Vector

We condition the discriminator on a vector w , containing various information about the input image. In particular, the type of input data (head, chest, abdomen or leg) is provided, in addition the slice interval (4mm or 8mm), and the scale of the standard deviation σ (2 scales) used for the Gaussian kernel which is treated as the slice thickness. In total, 8 channels are added as conditional information to the discriminator.

4 Experiments

For verification of the proposed method, we use Peak Signal-to-Noise Ratio (PSNR) and Structural Similarity Index Metric (SSIM) [13] as automatic metrics. There is a huge gap between PSNR and human perception sense, thus do not always present reasonable result. SSIM is more reasonable measure in super resolution field, however there is still a gap to human perception sense. Therefore, as additional experiment, we conducted Visual Turing Test (VTT). We asked 8 people who is either radiology technician or medical image research scientist to select the most high visibility image generated from 4 different methods each input. In the VTT, 4 images are shown in random order for 50 times to aggregate the answered ratio.

4.1 Datasets and Data Augmentation

We prepared 354 CT data (head:99, chest:98, abdomen:100, legs:57) for training which are obtained from diverse manufacturer’s equipments (*e.g.*, GE, Siemens, Toshiba, etc). They have been carefully selected to not contain metal artifacts or noises because the discriminator is prone to reproduce such artifacts. The input images CT values are clipped to the $[-2048, 2048]$ range and then normalized to be in the $[-1, 1]$ interval. In general, thick CT images are acquired in the range of 3-10 mm interval. On the other hand, 1mm slice interval is enough for 3D visualization of principle anatomy by volume rendering. We set the experimental setting to generate 1 mm slice interval images from 8 mm. Therefore our datasets are only data with smaller than 1.0 mm slice interval. All images are rescaled to 1mm isotropic voxels in preprocessing steps. In each training iteration, we randomly crop $160 \times 160 \times 160$ voxels from the input data and apply data augmentation. In particular, we apply an affine transformation consisting of a random rotation between -5 and +5 degrees, and random scaling between -5% and +5%, both sampled from uniform distributions. The generated thick slice image inputs are subject to Gaussian filtering with σ uniformly sampled between 0.0 and 3.2 voxels before being downsampled to 1/4 or 1/8 resolution. As test datasets, we prepared 53 CT data (head:12, chest:16, abdomen:15, leg:10).

4.2 Results

We report for reference methods adapted to 3D, including bicubic, SRCNN [3], Pix2Pix [7], and Virtual Thin Slice (VTS, our approach). For our approach we

Table 1. PSNR and SSIM comparison result in experiments.

Methods	GANs	Conditional?	HF prediction?	PSNR	SSIM
Bicubic				32.34	0.878
SRCNN [3]				33.73	0.904
Pix2Pix [7]	✓			35.14	0.925
VTS (ours)	✓	✓	✓	35.73	0.933
(w/o) condition	✓		✓	35.17	0.924
(w/o) HF pred.	✓	✓		33.70	0.905
Ground Truth	-	-	-	∞	1.000

perform an ablative study where we remove the conditional vector from the discriminator and high-frequency component prediction. We employ SRCNN’s 3 layer 9-1-5 model with each kernel expanded to 3D. Pix2Pix’s convolutional networks are also replaced to $4 \times 4 \times 4$ sized kernels in each layer to adapt 3D and iterates down sampling until the feature image size become one pixel. Each type of network architecture is trained for around 100 epochs with Adam optimizer having learning rate for 2×10^{-4} and momentum parameter $\beta_1 = 0.5$.

Table 1 shows average PSNR and SSIM calculated over the test datasets. VTS has the highest score among other methods and the ablation study shows that removing either the conditional vector or high-frequency prediction lowers the quality of the generated outputs.

As we can see in Figure 4, proposed VTS model generated the best perceptual quality with more sharpness and realistic images than other models. In particular, VTS works better with high intensity values such as bone boundary area rather than soft tissues. Although Pix2Pix model has similar PSNR/SSIM score to VTS, VTS was preferred roughly 90% of the time in VTT presented as shown in Figure 5. The boxplot shows the answered ratio among 4 methods by the research participants. The images in which Pix2Pix was preferred over VTT consists primarily of legs data which have small difference between thick and thin as shown bottom row in Figure 4. Even with some test data containing metal artifacts and unknown test patterns, the generated images are consistent with the input patterns, and don’t contain enhancing artifacts or noise.

Another important feature of the proposed method is that the generator network is a fully convolutional neural network, and as such can handle each part of body and also field of view. Additionally, we have performed a verification test on 66 real thick slice images covering a wide condition of view with varying slice numbers (10 to 327), slice intervals (from 3.0 to 10.0 mm), and FOV (128 to 512 mm*mm). Using this dataset, we confirmed that the generator networks are able to successfully generate 1mm slice interval images from the diversity of slice spacing and FOV images. We attribute these results to the wide range of data augmentation that we apply during training. Example of generated HR image from real existing thick slice image for either whole body or chest are shown in Fig. 1. The entire images are naturally reconstructed with no seams.

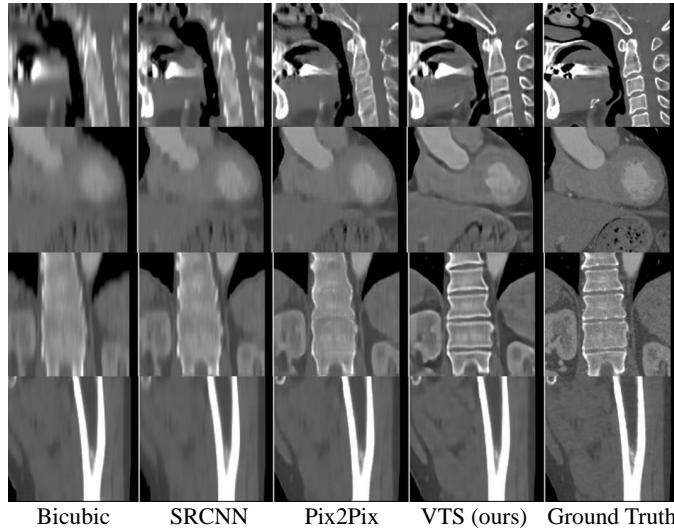


Fig. 4. Comparison of the generated images of bicubic, SRCNN [3], pix2pix [7], VTS (ours) and corresponding ground truth thin slice image. [$8\times$ slice interpolation]

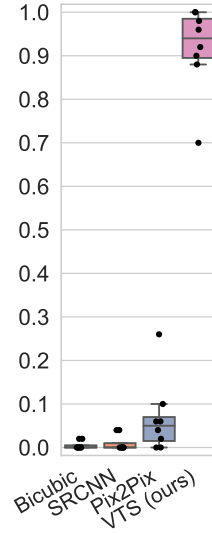


Fig. 5. The answered ratio in the Visual Turing Test.

5 Conclusion

In this paper, we have presented a super resolution algorithm that can be applicable for CT images of main body parts and various field of view. By inputting additional information regarding input data in the discriminator network, we show that output data quality increases significantly. Furthermore, the additional information is not necessary as test time. Numbering vertebrae bone is clearly easier with our VTS images compared to the original thick images. Also, we believe in-depth evaluation on abnormal images is an important next step for future work. In the future, we expect our VTS method will take on a role for the further development of medical image analysis and diagnosis support tasks, such as bone labeling and lung section segmentation, for thick slice data.

References

1. Blau, Y., Michaeli, T.: The perception-distortion tradeoff. In: Proceedings of the IEEE Conference on Computer Vision and Pattern Recognition. pp. 6228–6237 (2018)
2. Chen, Y., Shi, F., Christodoulou, A.G., Xie, Y., Zhou, Z., Li, D.: Efficient and accurate mri super-resolution using a generative adversarial network and 3d multi-level densely connected network. In: International Conference on Medical Image Computing and Computer-Assisted Intervention. pp. 91–99. Springer (2018)

3. Dong, C., Loy, C.C., He, K., Tang, X.: Learning a deep convolutional network for image super-resolution. In: European conference on computer vision. pp. 184–199. Springer (2014)
4. Duchon, C.E.: Lanczos filtering in one and two dimensions. *Journal of applied meteorology* **18**(8), 1016–1022 (1979)
5. Goodfellow, I., Pouget-Abadie, J., Mirza, M., Xu, B., Warde-Farley, D., Ozair, S., Courville, A., Bengio, Y.: Generative adversarial nets. In: Advances in neural information processing systems. pp. 2672–2680 (2014)
6. Ioffe, S., Szegedy, C.: Batch normalization: Accelerating deep network training by reducing internal covariate shift. arXiv preprint arXiv:1502.03167 (2015)
7. Isola, P., Zhu, J.Y., Zhou, T., Efros, A.A.: Image-to-image translation with conditional adversarial networks. arXiv preprint (2017)
8. Ledig, C., Theis, L., Huszár, F., Caballero, J., Cunningham, A., Acosta, A., Aitken, A., Tejani, A., Totz, J., Wang, Z., et al.: Photo-realistic single image super-resolution using a generative adversarial network. arXiv preprint (2017)
9. Metz, L., Poole, B., Pfau, D., Sohl-Dickstein, J.: Unrolled generative adversarial networks. arXiv preprint arXiv:1611.02163 (2016)
10. Mirza, M., Osindero, S.: Conditional generative adversarial nets. arXiv preprint arXiv:1411.1784 (2014)
11. Radford, A., Metz, L., Chintala, S.: Unsupervised representation learning with deep convolutional generative adversarial networks. arXiv preprint arXiv:1511.06434 (2015)
12. Ronneberger, O., Fischer, P., Brox, T.: U-net: Convolutional networks for biomedical image segmentation. In: International Conference on Medical image computing and computer-assisted intervention. pp. 234–241. Springer (2015)
13. Wang, Z., Bovik, A.C., Sheikh, H.R., Simoncelli, E.P.: Image quality assessment: from error visibility to structural similarity. *IEEE transactions on image processing* **13**(4), 600–612 (2004)
14. Yang, C.Y., Ma, C., Yang, M.H.: Single-image super-resolution: A benchmark. In: European Conference on Computer Vision. pp. 372–386. Springer (2014)
15. Zhang, H., Goodfellow, I., Metaxas, D., Odena, A.: Self-attention generative adversarial networks. arXiv preprint arXiv:1805.08318 (2018)

Acknowledgements

We acknowledge using the Reedbush-L (SGI Rackable C2112-4GP3/C1102-GP8) HPC system in the Information Technology Center, The University of Tokyo for the GPU computation required in this work.

Appendix

We include a variety of additional generated images from proposed VTS and other methods in Figure 6.

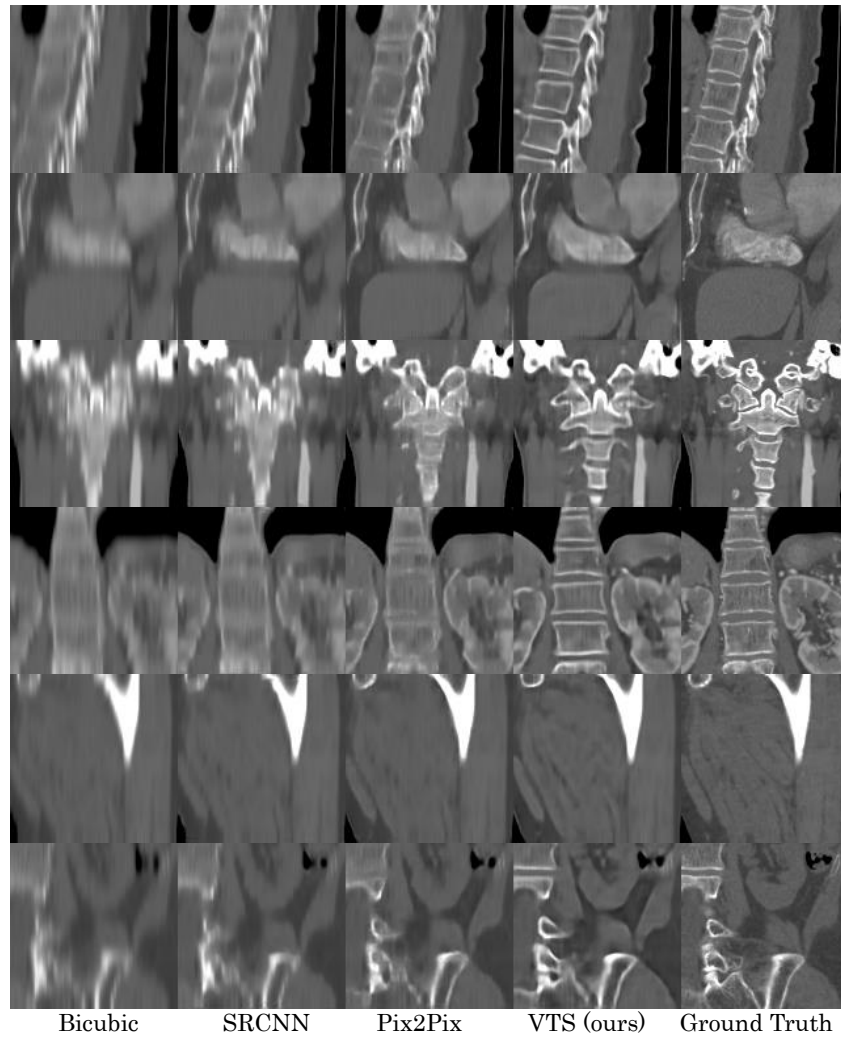


Fig. 6. Results using bicubic, SRCNN [3], pix2pix [7], VTS (ours) and corresponding ground truth thin slice image.